AD-A067 930 SCOTT POLAR RESEARCH INST CAMBRIDGE (ENGLAND) F/G 8/12
CHARACTERISTICS OF DEEP PRESSURE RIDGES IN THE ARCTIC OCEAN,(U)
1978 P WADHAMS N00014-76-C-0660
UNCLASSIFIED NL

| OF |
ADA
067930

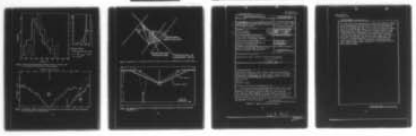

END
DATE
FILMED
6-79
DDC

Scott Polar Research Institute

see back page for 1473

CHARACTERISTICS OF DEEP PRESSURE RIDGES IN THE ARCTIC OCEAN

Peter Wadhams

CHARACTERISTICS OF DEEP PRESSURE RIDGES IN THE ARCTIC OCEAN

Peter Wadhams
Scott Polar Research Institute
Cambridge, England

1. INTRODUCTION

The deepest pressure ridges in an icefield are of particular interest to engineers and glaciologists. When an icefield is advected into shallow water the deepest keels are the first to take the ground and so determine the extent of sea bottom scouring. Oil drilling platforms must be built to withstand the impact of the largest ridges that are expected to exist in their area, and the design of polar icebreakers requires a knowledge of the strengths and sizes of the largest ridges that occur at a high enough frequency to be unavoidable. In the Arctic Ocean the deepest keels add greatly to the form drag of the ice cover, and may cause wave drag by generating internal waves (Hunkins, 1974). Kinematic models simulating ridge growth have been developed (Parmerter and Coon, 1972) in which a strip of rubble (formed by the collapse of thin ice within a lead) is allowed to be crushed between two converging ice sheets. The unsymmetrical piling of the rubble above and below the sheets causes progressive bending failure of the sheets, and the broken blocks add to the rubble to build the ridge. An examination of deep keel shapes and maximum drafts provides the data to test such kinematic models. The present study is an analysis of all keels of 30 m draft or greater found during a 3900 km sonar profile of the Arctic Ocean.

The profile was obtained in October 1976 during a co-operative experiment involving the British nuclear submarine HMS SOVEREIGN and an Argus aircraft of Maritime Command, Canadian Forces. The submarine recorded an upward-looking sonar profile while the aircraft flew along an identical track during the same period using a laser profilometer to record ice surface elevation (Wadhams, 1977a; Wadhams and Lowry, 1977). The main aim of the experiment was to derive statistical relationships between the surface and bottom topography of the ice by comparing corresponding sections of sonar and laser profile (Wadhams, 1977b). A causal point-to-point comparison of the profiles is not possible because of mutual navigation errors. The sonar profile was recorded on Teledeltos paper using a Kelvin Hughes MS45 echo sounder feeding a 45 kHz transducer with overall beamwidths to the 3 dB points of 17^{o} fore-and-aft and 5^{o} athwartships. The chart record scales were 2 m: 10 mm in the vertical plane and 1 minute: 75 mm in the horizontal plane. This gave considerably better resolution than the recorders used in earlier profiling experiments (Lyon, 1961; Swithinbank, 1972), especially when the submarine cruised slowly. Fig.1 shows a keel of 35.7 m draft and width at least 600 m recorded at a speed of 7 knots (3.6 m s^{-1}). The effect of the fore-and-aft beamwidth is seen in the individual hyperbolae surrounding strong reflecting points on the ridge, but in general the shape of the keel is well reproduced. The sonar profile is thus a

valuable data source on individual under-ice features.

Independent keels exceeding 30 m in draft were identified using a transparent overlay and a Rayleigh selection criterion (Williams et al, 1975) whereby a keel is deemed independent if the troughs on either side of the crest regress at least half way towards the local draft of level ice. Sea level could be estimated to ± 20 cm by interpolation between the nearest open cracks on either side of the keel, since the submarine's depthkeeping was excellent and open water revealed itself clearly by giving multiple sonar echoes. Each keel was then traced from the chart record, the ridge being considered to exist as an entity until either

a) the ice draft dropped below 5 m, or
b) the draft reached a minimum from which it began to rise to form a new independent keel.

2. THE DISTRIBUTION OF KEEL DRAFTS

45 independent deep keels were found in 3907 km of track, an average of one keel per 87 km. The distribution of drafts was as follows:-

30-32 m	24 keels	36-38 m	4 keels
32-34 m	11 keels	38-40 m	1 keel
34-36 m	4 keels	40 m +	1 keel

The deepest keel (no.39 in fig.3) was the only one whose draft exceeded the scale limit of the recorder (40 m) so that its peak was lost. From extrapolation of the slopes it is conservatively estimated to have a draft of 42-43 m. The deepest keel yet recorded in the Arctic Ocean had a draft of 47 m (Lyon, quoted by Weeks et al, 1971).

Hibler et al (1972) proposed a theoretical ridge height distribution which has been extensively tested against observation. The probability density P(h) was obtained by finding the most likely distribution of ridges that will yield a given volume of deformed ice assuming that all ridges are geometrically congruent. It is given by

$$P(h)\,dh = 2\kappa \bar{h} \exp(\kappa h_o^2) \exp(-\kappa h^2)\,dh \qquad (1)$$

where $\bar{h}$ is the mean draft, h_o is a low value cutoff and κ is a parameter which must be derived iteratively from the relationship

$$\exp(-\kappa h_o^2) = \bar{h}\,(\kappa\pi)^{\frac{1}{2}}\,\mathrm{erfc}(\kappa^{\frac{1}{2}} h_o) \qquad (2)$$

To estimate the fit of the deepest keels to (1) it was necessary to measure over a much larger range of depths, so the transparent overlay technique was used to find the numbers of independent keels with drafts greater than 10 m in 5 m intervals. 8367 ridges were found (2.14 per km) and fig.2 shows the observed and theoretical distributions plotted on a log-lin histogram. The parameters were:- κ = 0.006, h_o = 10, $\bar{h}$ = 14.45. There is an excellent fit between theory and observation for all the moderate depth classes, showing the essential validity of Hibler's theory. However, at drafts exceeding 30 m the observed numbers of keels definitely exceed the theoretical predictions. The numbers are:-

30-35 m	37 observed	27.3 predicted
35-40 m	7 observed	3.5 predicted
40 m +	1 observed	0.3 predicted

It is noteworthy that existing tests of (1) against observation (Hibler et al, 1972; Hibler, 1975) used short lengths of track in which the higher depth classes were pooled together in order to attain a statistically reasonable number of keels. Any deviation from theory at the extreme tail of the distribution therefore would not be

detected. The present profile is the longest to be tested against theory, so until further evidence is available we must assume that there is a significant positive deviation of observation from theory for ice keels beyond 30 m in draft. Thus the engineer who wishes to use (1) to estimate the frequency of very deep keels in an icefield by extrapolation from limited data must exercise caution, and for safety's sake should increase his estimates of deep keel frequencies by 50-100%.

3. THE GEOGRAPHICAL DISTRIBUTION OF DEEP KEELS

Fig.3 shows all 45 deep keels plotted along the submarine's track chart. The geographical distribution reflects the division of the Arctic into ridging zones proposed by Weeks et al (1971) and analysed, for the SOVEREIGN data, by Wadhams and Lowry (1977). Weeks et al identified an "offshore zone" of very heavy ridging stretching some 250 km from the north coasts of Greenland and the Canadian Archipelago into the Arctic Ocean. This is followed by the "central Arctic" zone of milder ridging. Wadhams and Lowry found heavy ridging along the submarine's westward track from 82°N to 85°N 70°W, with the most intense ridging being near this turning point and for the first 200 km of the northward leg towards the Pole. At 87°N there is an abrupt transition to milder ridging which prevails until the Greenland coast is approached again. The distribution of the deepest keels follows the same pattern. Within the central Arctic zone (from 87°N 70°W northward to the Pole and down to the position of ridge 40) there are only 5 deep ridges in 2000 km of track, whereas in the offshore zone (from 82°N west to 70°W and north to 87°N 70°W) there are 39 deep ridges in 1050 km. The lightly ridged area is the Trans Polar Drift Stream, which carries mainly first- and second-year ice across the Eurasian Basin from Siberia down towards the East Greenland Current. The heavy ridging occurs when the Drift Stream's approach to the coast of Greenland causes convergence in the ice cover and consequent deformation. At 70°W the Drift Stream has given way to the Beaufort Gyre, containing mainly older ice, and the deformation of this older ice against the coast produces the especially intense ridging in that area.

There is also a statistically significant clustering effect in the geographical distribution. This is seen especially in ridges 1 and 40-44; 14-20; 22-25; 26-30; and 31-34. The clusters in the 70°W region are shown more clearly in fig.4. Ridges 14-20, for instance, are all contained within a triangle of side 16 km, while 26-28 are spaced only 1 km apart. The first possibility is that each cluster represents a single ridge sampled at several points; such a ridge would have a very sinuous shape. It is quite possible that a closely spaced pair can be explained in this way, and as an overall explanation it cannot be rejected in the absence of two-dimensional information on ridge orientations. However, it is more likely that a cluster of very deep keels is a relic of a single past event of intense convergence in which one or more long, deep keels were formed. In the subsequent deformation of the ice cover the long ridges were split into independent linkages which drifted and revolved relative to one another while remaining in reasonably close company. In practical terms, e.g. to an icebreaker captain, the clustering effect implies that if a very deep ridge is encountered there are likely to be others not far away.

4. THE SHAPES OF DEEP KEELS

(i). Observed profiles

Many careful measurements have been made of the subsurface shapes of pressure ridges, using drilling techniques or sonar profiling from the side (e.g. Wittmann and Schule, 1966; Weeks et al, 1971; Kovacs, 1972; Kovacs et al, 1973). All authors agree that no

simple geometrical model is adequate to describe all ridges, and that even the concept of "slope angle" cannot be applied to some multi-year ridges with bowl-shaped or semi-elliptical keels (Kovacs et al, 1973). Measurements made from the ice sheet have the advantage that a true orthogonal cross-section of the ridge can be obtained. In the SOVEREIGN profiles each ridge has an unknown orientation so that the observed slope angle is always less than the true slope; the sonar beamwidth reduces the observed slope still further. Nevertheless, the number of ridges in the sample permits some tentative statistical conclusions to be drawn.

Fig.5 shows a representative selection of keel profiles, drawn without vertical exaggeration but on various scales. The first three ridges (10, 15 and 19), drawn on the largest scale, have simple triangular topography. The slopes are virtually constant, and the apparent flattening of the crest can be largely explained by the effect of sonar beamwidth (eqn.5). Ridges 1 and 29 show more distinct flattening of the crest. The experiment was carried out in mid-October so that most, if not all, of the ridges have experienced at least one summer melt period and hence qualify as multi-year ridges. They are extremely strong on account of the refreezing of summer meltwater into the voids which previously existed between rubble blocks. Their crests have become rounded by summer melting and by erosion due to shear currents, which proceeds more rapidly in summer and which can transport entire ice blocks (Rigby and Hanson, 1976). Ridges 13, 27 and 39 have steep initial slopes leading to gently rounded crests. This may be the result of erosion of the crest, or it may be an example of a process described by Parmerter and Coon (1972), who postulated a maximum keel draft which is a function of the strength of the ice, the density of the rubble blocks in the ridge and the thickness of the ice sheet. Once a keel has reached its maximum draft further compression leads to a lateral growth into a wide, flat-bottomed hummock. Ridge 43 appears a well-developed example of this. Ridge 39, the deepest keel, is assumed to have a similar shape- otherwise its draft may be even greater than 43 m. Ridges 21, 25, 28 and 30 have been traversed at an acute angle so that the sonar is sampling along the keel crest rather than across it. The ultimate case is ridge 6 (see also fig.1), where over 600 m of the keel have been profiled.

From each ridge profile a pair of slope angles was estimated. Fig.5 shows that this can be a difficult undertaking, and a definite procedure was used. The region within $\pm$ 10 m range of the crest was ignored as possibly subject to sonar distortion. The remainder of the half-ridge was sampled as far as the point at which the slope changed radically- usually becoming more gentle but sometimes (e.g. ridge 27) becoming more steep. A linear regression was made on equally spaced points along this part of the keel- thus the slope is measured from the deeper part of the keel profile. 88 values were obtained (one keel was impossible to estimate) and their distribution is shown in fig.6. Slopes vary from almost zero to 51°, but with a concentration around $16\text{-}28^{\circ}$. The mean slope is 23.9°.

Another estimate of mean slope was made by drawing a "composite ridge" (fig.7), an amalgam of all ridges, in which depth points, normalised as fractions of the keel draft, were taken from the keel tracings and averaged in bins of width 4 m. A is the two-sided composite drawn out to a range of 80 m, beyond which the shallower keels cause the composite ridge to become almost flat. Since there is no reason to expect any left-right bias (assuming that the centre of the sonar beam was vertical), ridge A was itself averaged into a one-sided composite ridge B. This ridge consists of a flattened crest (probably an artefact); a steep initial slope (a) of angle 26.8° extending from 6 to 16 m from the crest; and a gentler slope (b) of angle 17.7° extending out to about 50 m. The angles were calculated by taking the depth of the composite keel as the mean draft of all the keels.

(ii). Theoretical slope angle distribution

Several geometrical shapes have been suggested as approximations to a typical keel profile. The simplest is the isosceles triangle proposed by Makarov in 1901 (Zubov, 1945) to describe new ridges; as the ridge ages the shape progresses by erosion and melting into a semi-ellipse. Intermediate between these extremes is the Wittmann and Schule (1966) model of an isosceles triangle with a rounded crest.

Figures 6 and 7 show slopes which are biased by the angle at which the ridge is crossed and by the effect of sonar beamwidth. We can estimate a true slope distribution from the data of fig.6 provided we make two assumptions:-

(a) that keels have random orientations- implying that keels oriented at right angles to the submarine's track will be sampled relatively more frequently than keels lying nearly parallel to the track;
(b) that a true cross-section through all keels will give the same geometrical shape. The simplest shape to choose is the Makarov model of an isosceles triangle with slope angle α.

If the submarine's track is oriented at an angle θ to a true cross-section, i.e. at $(\pi/2 - \theta)$ to the line of the keel (fig.8), the slope angle β encountered by the submarine is given by

$$\tan\beta = \cos\theta \tan\alpha \qquad (3)$$

The beamwidth of the transducer further distorts the slope. For simplicity we shall ignore the small athwartships beamwidth, and assume that SOVEREIGN's sonar had only a fore-and-aft beamwidth of half-angle λ ($\lambda = 8.5^{o}$). The observed profile generated by the first return from each sound pulse is shown in fig.9. Here D is the depth of the submarine below the ambient level ice draft (D = 72 m) and h is the depth of the keel below the same datum. The transit time of a sound pulse is neglected. The recorded profile gives the keel a greater apparent width, a reduced slope angle γ and a rounded crest, although the absolute draft of the crest is correctly recorded. The additional half-width x_o of the keel is given by

$$x_o = D\left[\sin\lambda - \cot\beta\ (1 - \cos\lambda)\right] \qquad (4)$$

and the lateral range x_1 to which the apparent rounding of the crest extends is given by

$$x_1 = (D - h)\tan\lambda \qquad (5)$$

which is about 5-6 m for h = 30-40 m. The apparent slope angle γ is given by

$$\tan\gamma = \frac{\sin\beta}{\cos(\beta - \lambda)} \qquad \beta > \lambda \qquad (6)$$

or

$$\tan\gamma = \sin\beta \qquad \beta \leq \lambda \qquad (7)$$

since when $\beta \leq \lambda$ the first return from a pulse is a specular reflection from the ridge slope, whereas when $\beta > \lambda$ the first return comes from the leading edge of the beam footprint.

Under our assumption (a) the probability density function of θ is given by

$$P(\theta)\, d\theta = \cos\theta\, d\theta \qquad (8)$$

Equations (3), (6) and (7) yield the transformations from θ to γ:-

$$\cot\gamma = \cos\lambda \sec\theta \cot\alpha + \sin\lambda \qquad \gamma > \gamma_o \qquad (9)$$

$$\cot\gamma = \sec\theta \cot\alpha \sqrt{1 + \cos^2\theta \tan^2\alpha} \qquad \gamma \leq \gamma_o \qquad (10)$$

where γ_o, the angle at which $\beta = \lambda$, is given by

$$\gamma_o = \tan^{-1}(\sin\lambda) \tag{11}$$

Thus the probability density function for γ is

$$P(\gamma)\, d\gamma = P(\theta)\left|\frac{d\theta}{d\gamma}\right| d\gamma = \frac{\operatorname{cosec}^2\gamma}{(\cot\gamma - \sin\lambda)} \frac{f^2}{(1-f^2)^{\frac{1}{2}}}\, d\gamma \qquad \gamma > \gamma_o \tag{12}$$

or

$$P(\gamma)\, d\gamma = \frac{\cot^2\alpha \tan 2\gamma}{2\left[\cos 2\gamma\ (\cos 2\gamma - \sin^2\gamma \cot^2\alpha)\right]^{\frac{1}{2}}}\, d\gamma \qquad \gamma \leq \gamma_o \tag{13}$$

where

$$f = \frac{\cos\lambda \cot\alpha}{(\cot\gamma - \sin\lambda)} \tag{14}$$

$P(\gamma)$ is the function which is sampled in fig.6 provided α takes only one value. The mean apparent slope angle $\bar{\gamma}$ is given by

$$\bar{\gamma} = \int_0^{\gamma_{max}} \gamma\, P(\gamma)\, d\gamma \tag{15}$$

where γ_{max}, the maximum apparent slope angle occurring when $\theta = 0$, is given by

$$\gamma_{max} = \tan^{-1}\left[\frac{\sin\alpha}{\cos(\alpha-\lambda)}\right] \tag{16}$$

from (6).

Equations (12) to (15) were solved numerically, and a typical curve of $P(\gamma)$ is shown in fig.10, using $\alpha = 33^o$, the average slope angle for first-year keels found by Weeks *et al* (1971) and Kovacs (1972). This agrees closely with an average value of 32^o given by Wittmann and Schule (1966). The probability increases rapidly near γ_{max} ($= 30.9^o$), giving $\bar{\gamma} = 27.0^o$. The shape of the curve does not agree with fig.6, showing that a single value for α is inadequate to describe the distribution of apparent slopes. It is clear that fig.6 is actually a convolution of $P(\gamma)$ with $P(\alpha)$, the probability density function for α. To evaluate $P(\alpha)$ we must deconvolve fig.6. This was done numerically as follows. The bin with the highest slope angles (48-52^o) was emptied by postulating a number $n(\alpha)$ of ridges with α such that $\gamma_{max} = 52^o$ and with n sufficient to produce the required number of ridges with apparent slopes of 48-52^o using the results of (12)-(15). The contributions made by n to all the other bins were then calculated. The process was then repeated for the next lowest bin (44-48^o), having made allowance for the number already described by the first $n(\alpha)$. Thus all bins were emptied successively in descending order. The distribution of $n(\alpha)$ has been added to fig.6; this is now the distribution of true ridge slopes. The slope angles vary from 8^o to 56^o; the average slope angle is 32.1^o. This happens to be in excellent agreement with the average values quoted by other researchers.

The agreement is pleasing but possibly fortuitous, since the deconvolution process involves a large step size. Having shown that this type of calculation is feasible, we now plan to apply it to the whole digitised SOVEREIGN profile, carrying out automatic slope analyses on keels of lower draft than 30 m. The vastly greater numbers of such ridges will increase the reliability of the probabilistic technique described above.

5. SUMMARY

An examination has been carried out of 45 pressure ridge keels with draft exceeding 30 m found during a submarine transit of the Arctic Ocean. This is the largest number of keels yet studied in this way. A probabilistic technique has been developed

to derive the true distribution of slope angles from the observed distribution, and the average slope angle was found to be 32.1°, in close agreement with averages found by experimenters who have worked on ridges (all shallower than 30 m) *in situ*. Thus there is no evidence for a significant difference in average slope between deep keels and shallow keels. The deep keels vary greatly in shape, progressing from a simple triangle to flattened bowls and more complex shapes. Their geographical distribution is similar to that of shallower ridges, but with a greater relative difference in ridge frequency between heavily and lightly ridged areas. There is a distinct clustering effect, suggesting that a group of deep keels spreads from a single origin. There are significantly more deep keels than predicted by the theory of Hibler *et al* (1972); the deepest observed keel had a draft exceeding 42 m.

ACKNOWLEDGEMENTS

I wish to thank the captain and crew of HMS SOVEREIGN, whose skill resulted in a successful experiment; the Hydrographer of the Navy for the opportunity to participate in the cruise; and the Admiralty Underwater Weapons Establishment, Portland. I am also grateful to Mr. R.J. Boyle for assistance in data gathering, and to Miss M.P. Casarini and Mr. G. Winskel for data analysis. It is a pleasure to acknowledge the support of the Office of Naval Research under contract NO 0014-76-C-0660.

REFERENCES

Hibler, W.D. III, W.F. Weeks and S.J. Mock (1972). Statistical aspects of sea ice ridge distributions. *J. Geophys. Res.*, 77(30), 5954-5970.

Hibler, W.D. III (1975). Statistical variations in Arctic sea ice ridging and deformation rates. Proc. Ice Tech Symp., Montreal, 9-11 April 1975. Soc. Nav. Archit. Mar. Engrs., New York, J1-J9.

Hunkins, K. (1974). An estimate of internal wave drag on pack ice. *AIDJEX Bull.*, 26, 141-152.

Kovacs, A. (1972). On pressured sea ice. In *Sea Ice*, Proc. Int. Sea Ice Conf., Reykjavik, 10-13 May 1971. Nat. Res. Coun. of Iceland, 276-295.

Kovacs, A., W.F. Weeks, S. Ackley and W.D. Hibler III (1973). Structure of a multi-year pressure ridge. *Arctic*, 26(1), 22-31.

Lyon, W. (1961). Ocean and sea-ice research in the Arctic Ocean via submarine. *Trans. N.Y. Acad. Sci.*, 23(8), 662-674.

Parmerter, R.R. and M.D. Coon (1972). Model of pressure ridge formation in sea ice. *J. Geophys. Res.*, 77(33), 6565-6575.

Rigby, F.A. and A. Hanson (1976). Evolution of a large Arctic pressure ridge. *AIDJEX Bull.*, 34, 43-71.

Swithinbank, C.W.M. (1972). Arctic pack ice from below. In *Sea Ice*, Proc. Int. Sea Ice Conf., Reykjavik, 10-13 May 1971. Nat. Res. Coun. of Iceland, 246-254.

Wadhams, P. (1977a). A British submarine expedition to the North Pole, 1976. *Polar Rec.*, 18(116), 487-491.

Wadhams, P. (1977b). A comparison of sonar and laser profiles along corresponding tracks in the Arctic Ocean. Presented at ICSI/AIDJEX Conf. on Sea Ice Processes and Models, Seattle, 6-9 Sept 1977.

Wadhams, P. and R.T. Lowry (1977). A joint topside-bottomside remote sensing experiment on Arctic sea ice. Proc. 4th Can. Symp. on Remote Sensing, Quebec, 16-18 May 1977. Can. Remote Sensing Soc.

Weeks, W.F., A. Kovacs and W.D. Hibler III (1971). Pressure ridge characteristics in the Arctic coastal environment. Proc. 1st Int. Conf. on Port and Ocean Engng. under Arctic Conditions. Tech. Univ., Trondheim, 1., 152-183.

Williams, E., C.W.M. Swithinbank and G. de Q. Robin (1975). A submarine sonar study of the Arctic pack ice. J. Glaciol., 15(73), 349-362.

Wittmann, W.I. and J.J. Schule (1966). Comments on the mass budget of Arctic pack ice. Proc. Symp. Arctic Heat Budget and Atmos. Circ. RAND Corp., Santa Monica, Calif., Rep. RM-5233-NSF, 215-246.

Zubov, N.N. (1945). Arctic Ice. Izdatel'stvo Glavsermorputi, Moscow. Eng. Transln. by U.S. Naval Oceanogr. Off. / Am. Met. Soc. 491pp.

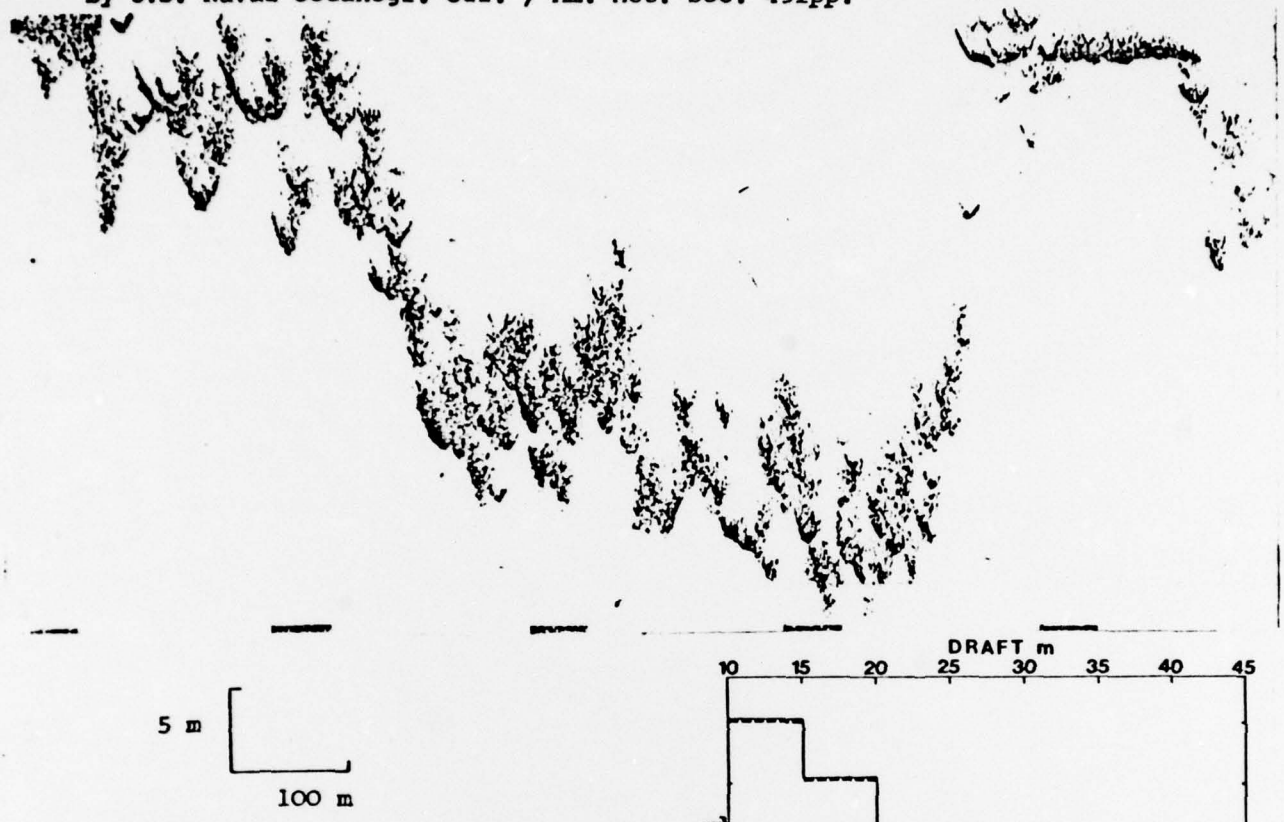

FIG.1 (above) Sonar trace of a deep Arctic pressure ridge keel (keel no.6; 84°40'N 35°43'W).

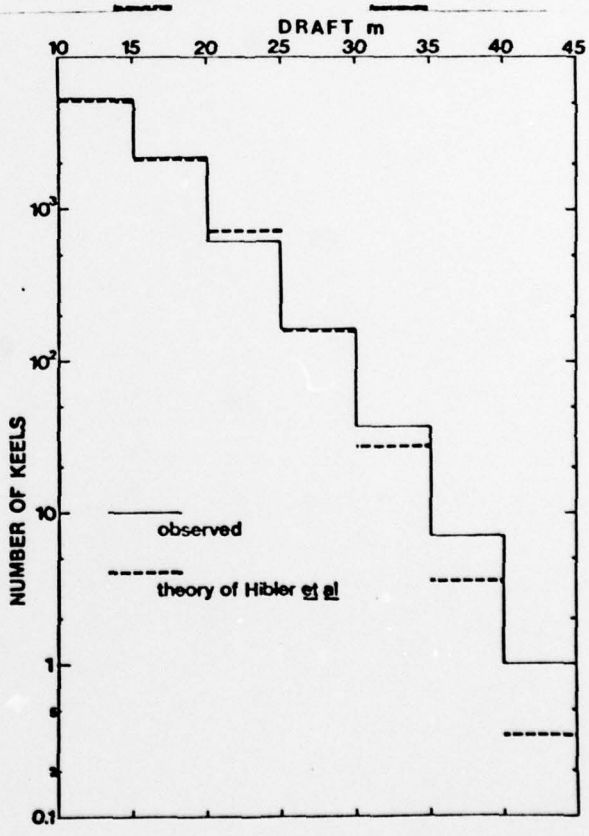

FIG.2 (right) Comparison of observed and theoretical keel frequencies.

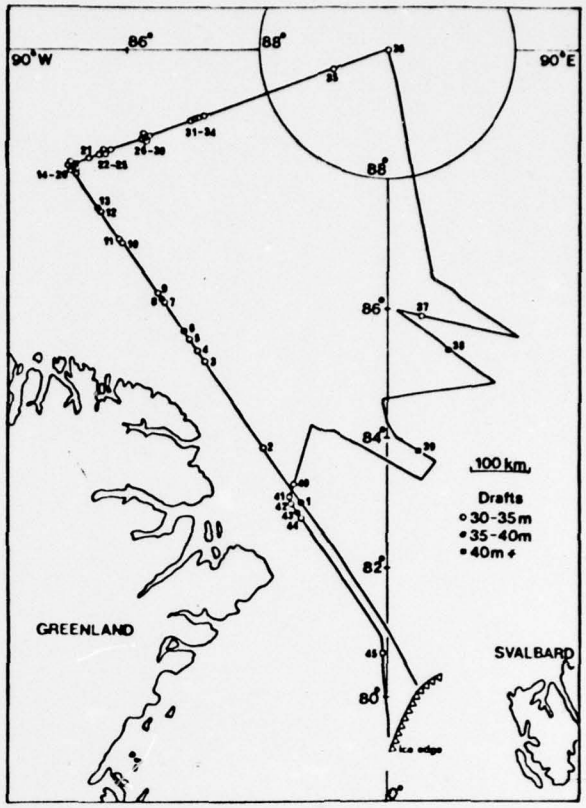

FIG. 3

Keels exceeding 30 m in draft plotted on track of SOVEREIGN

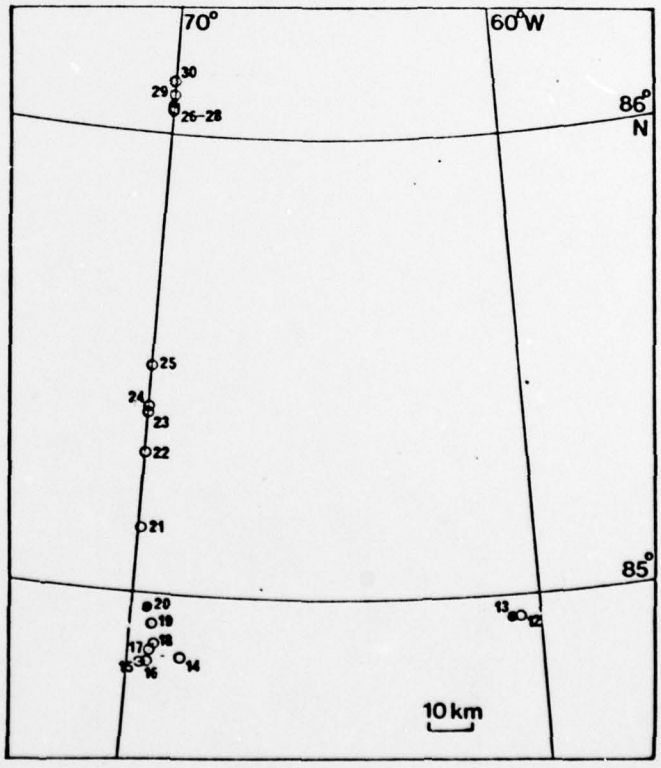

FIG. 4

Deep keels in vicinity of 70°W

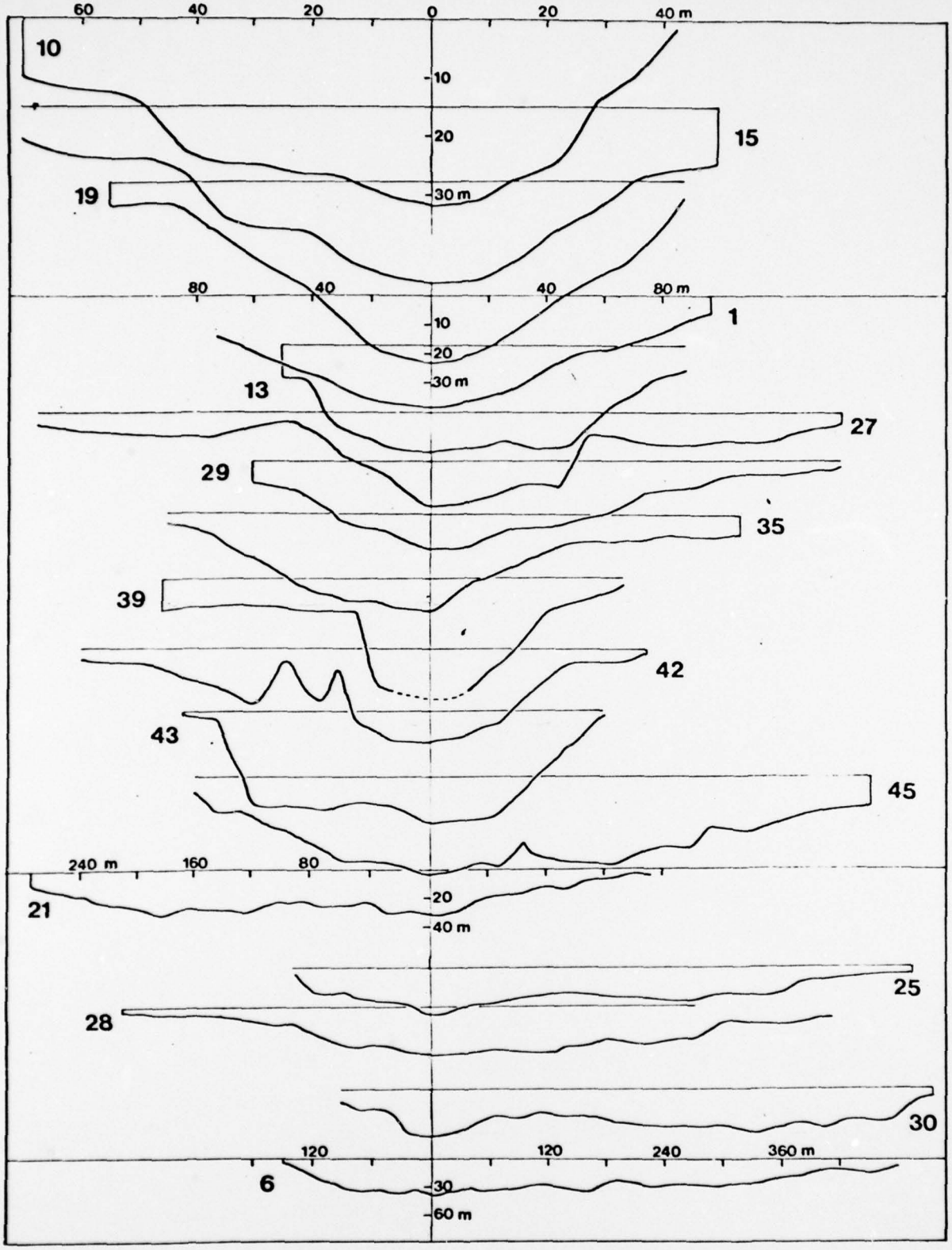

FIG.5 Representative profiles of deep keels. Range is measured from point of greatest draft.

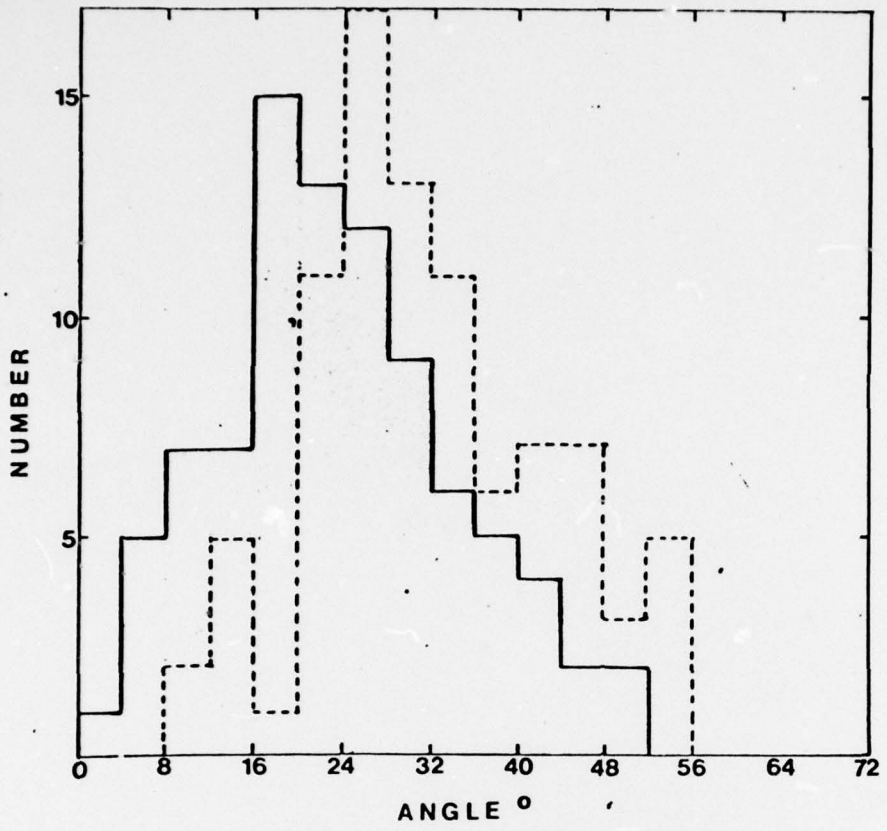

FIG.6 Observed distribution of slope angles. Dashed line is inferred distribution of true slopes.

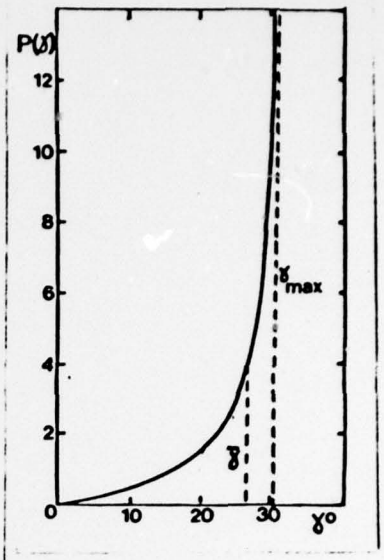

FIG.10 (above)

The function $P(\gamma)$ for $\alpha = 33^{\circ}$. $\gamma_{max} = 30.9^{\circ}$ $\bar{\gamma} = 27.0^{\circ}$.

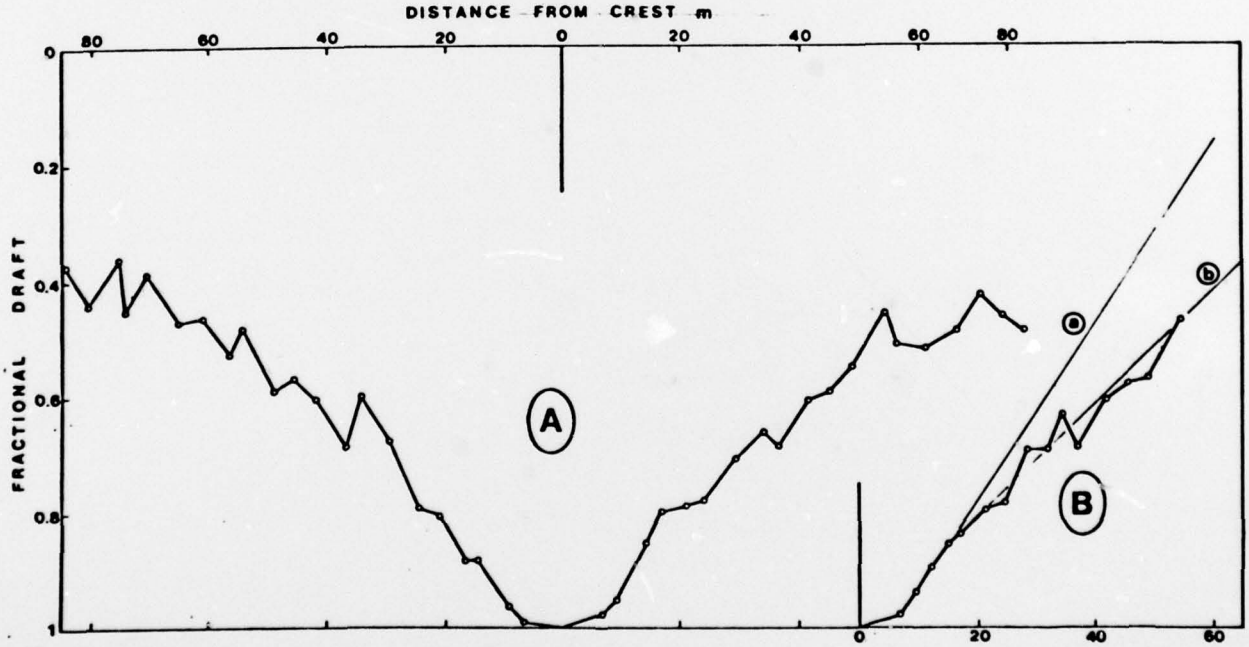

FIG.7 "Composite ridge" obtained by averaging all the normalized ridge profiles. B is average of two sides of A.

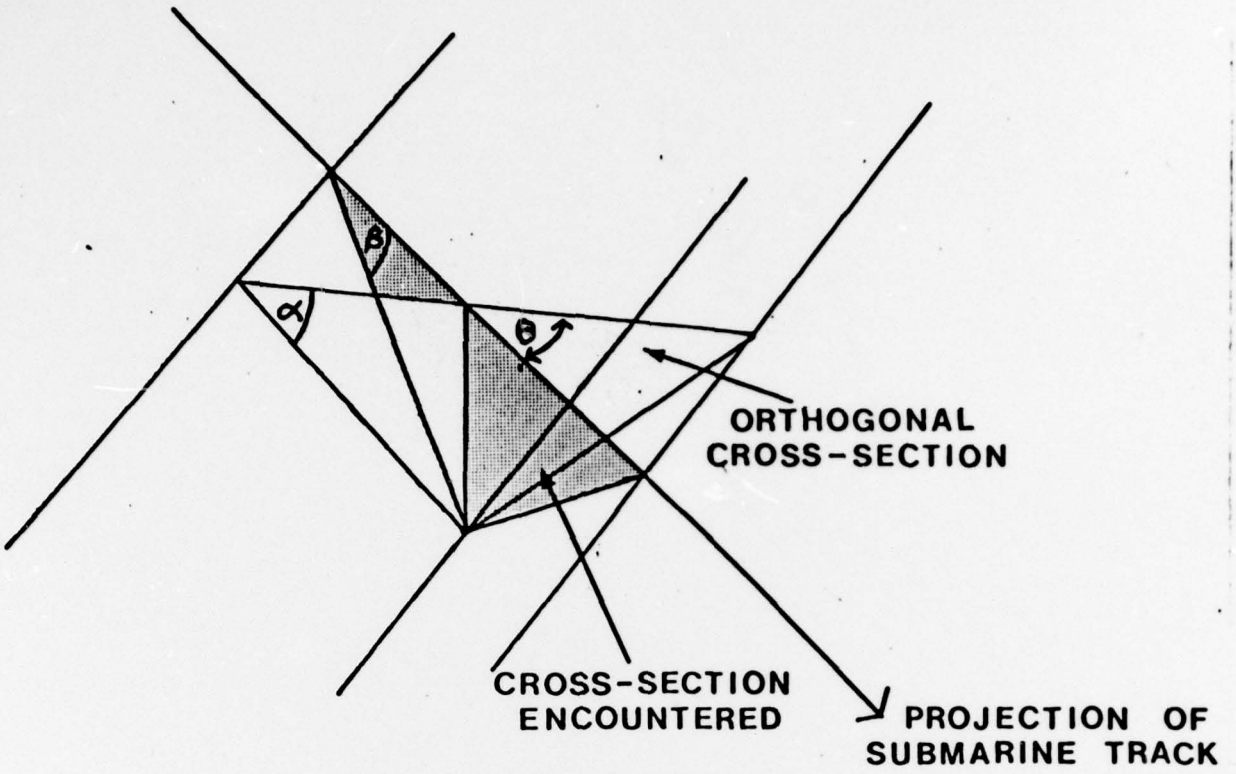

FIG.8 Geometry of a triangular keel of slope α cut by a submarine at a slant angle.

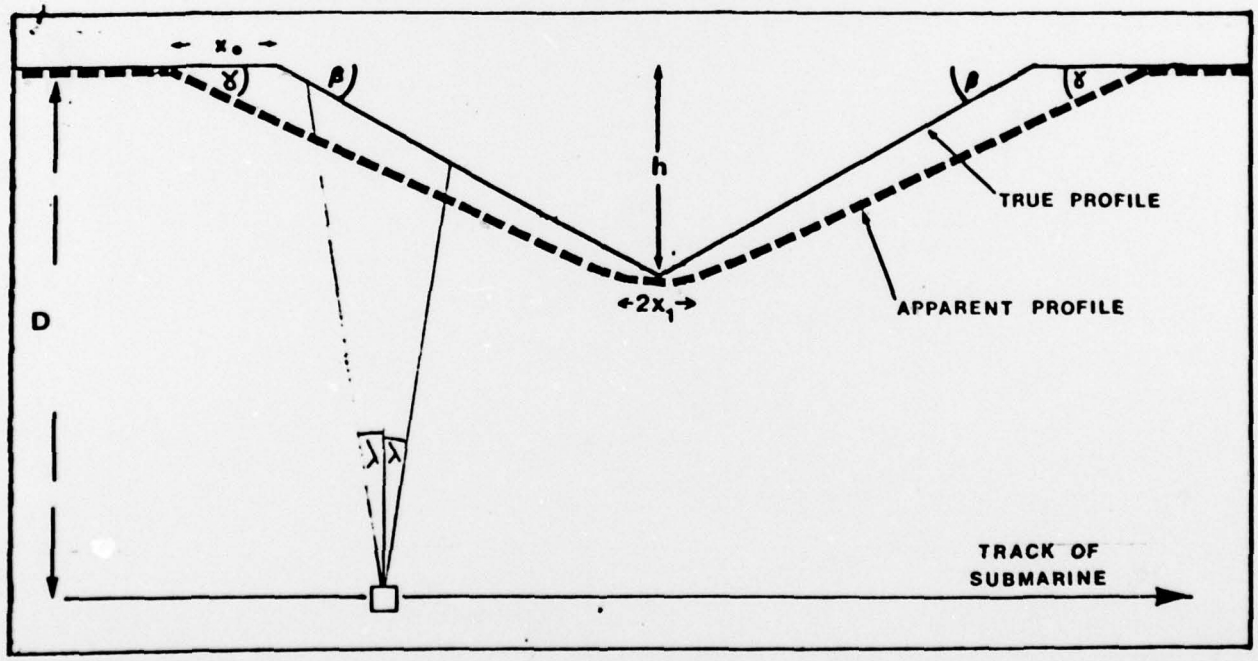

FIG.9 The apparent profile of a triangular keel recorded by a sonar with overall beamwidth 2λ.

Unclassified
SECURITY CLASSIFICATION OF THIS PAGE (When Data Entered)

REPORT DOCUMENTATION PAGE

READ INSTRUCTIONS BEFORE COMPLETING FORM

1. REPORT NUMBER
2. GOVT ACCESSION NO.
3. RECIPIENT'S CATALOG NUMBER

4. TITLE (and Subtitle)
(6) CHARACTERISTICS OF DEEP PRESSURE RIDGES IN THE ARCTIC OCEAN

5. TYPE OF REPORT & PERIOD COVERED
Research results, 1976

6. PERFORMING ORG. REPORT NUMBER

7. AUTHOR(s)
(10) Peter Wadhams

(15) CONTRACT OR GRANT NUMBER(s)
N00014-76-C-0660,
N00014-78-G-0003

9. PERFORMING ORGANIZATION NAME AND ADDRESS
Scott Polar Research Institute,
University of Cambridge, England

10. PROGRAM ELEMENT, PROJECT, TASK AREA & WORK UNIT NUMBERS

11. CONTROLLING OFFICE NAME AND ADDRESS
Office of Naval Research, Arctic Programs, Arlington, Va.

12. REPORT DATE
(11) 1978

13. NUMBER OF PAGES
12

14. MONITORING AGENCY NAME & ADDRESS (if different from Controlling Office)
Dept. of Oceanography, University of British Columbia, Vancouver B.C.

15. SECURITY CLASS. (of this report)
Unclassified

15a. DECLASSIFICATION/DOWNGRADING SCHEDULE

16. DISTRIBUTION STATEMENT (of this Report)
Approved for public release, distribution unlimited

(12) 16p.

17. DISTRIBUTION STATEMENT (of the abstract entered in Block 20, if different from Report)

18. SUPPLEMENTARY NOTES
Presented at 4th Intl. Conf. on Port and Ocean Engineering Under Arctic Conditions, St. John's, Nfld., Sept. 26-30 1977. Published in Proceedings (ed. D.B. Muggeridge), 1, 544-555.

19. KEY WORDS (Continue on reverse side if necessary and identify by block number)
Arctic Ocean
Sea ice
Pressure ridges

20. ABSTRACT (Continue on reverse side if necessary and identify by block number)
An examination has been carried out of 45 pressure ridge keels with draft exceeding 30 m that were found to occur in a 3900 km sonar profile of Arctic Ocean ice cover made by the submarine HMS SOVEREIGN in October 1976. The deepest keel was 43 m draft. The numbers of deep keels exceeded those predicted by the theory of Hibler et al (1972). Geographically

DD FORM 1 JAN 73 1473 EDITION OF 1 NOV 65 IS OBSOLETE

Unclassified
SECURITY CLASSIFICATION OF THIS PAGE (When Data Entered)

Figure 6. Report Documentation Page.

318 900

the deep keels were concentrated in the zone of heavy ridging off north Greenland and Ellesmere Island (one deep keel per 27 km on average), and were scarce in the central Eurasian Basin (one per 400 km). There is a distinct clustering effect, suggesting that a group of deep keels spreads from a single originating event. A probabilistic technique was developed to derive the true distribution of slope angles from the observed distribution, and the mean slope angle was found to be 32.1^{o}, in close agreement with direct measurements by other experimenters. The actual shapes of the deep keels vary widely, from a simple triangle to a flattened bowl and more complex shapes.